Jordan Journal of Civil Engineering, Volume **18**, No. **2**, **2024**
DOI: https://doi.org/10.14525/JJCE.v18i2.02

Jordan Journal of Civil Engineering

Journal homepage: https://jjce.just.edu.jo

An Integrated Geophysical Investigation for Detecting Seepage-prone Zones in the Basement of a Building

Sanjay Rana [1),2)], ***Varun Narayan Mishra*** [1)*], ***Praveen Kumar Rai*** [3)]

[1)] *Amity Institute of Geoinformatics and Remote Sensing (AIGIRS), Amity University, Sector 125, Noida 201313, India.*
[2)] *PARSAN Overseas Pvt. Ltd., New Delhi 110019, India. * Corresponding Author. E-Mails: vnmishra@amity.edu; varun9686@gmail.com*
[3)] *Department of Geography, Khwaja Moinuddin Chishti Language University, Lucknow 226013, India.*

ARTICLE INFO

Article History:
Received: 6/7/2023
Accepted: 25/1/2024

ABSTRACT

The underground basement of a building is highly affected by anomalous seepage problems. Detection of seepage-prone regions through and around buildings becomes a need in other to sustain their stability. It is of great importance as well to have targeted remedies. However, traditional methods for examining these areas are often destructive and expensive, compelling the use of non-destructive geophysical techniques. This work aims to utilize and demonstrate the hands-on application of ground penetrating radar (GPR) and self-potential (SP) methods as an innovative combination to study seepage-prone zones in the basement of a building. Simulated responses of various seepage zones have been generated based on several significant factors. For better visualization, all 2D radargrams of a block were combined to produce a 3D model using GPR Slice software to distinguish various features at different depths. Higher positive SP values show the presence of high moisture or seepage-prone regions. Conclusively, the combined geophysical method of GPR and SP is trustworthy for conducting a quick and effective inspection of seepage-prone regions and probable source points for detailed characterization of the basement of a building.

Keywords: GPR, SP, Geophysical methods, Seepage, Basement.

INTRODUCTION

The construction of underground living spaces became a reasonable choice for city dwellers due to the lack of land. Seepage is a common, but undesirable, phenomenon that endangers the function and may unfavourably impact the basement of a building (Ramteke, 2013). It poses significant challenges in urban infrastructures, mainly in underground spaces, like basements, that may extend beyond mere inconvenience. Seepage is commonly observed in city dwellings due to the high density of construction and limited land availability, which can lead to a range of serious issues. Additionally, seepage frequently advances to health hazards and the moisture’s existence fosters the growth of mould and mildew, which are acknowledged to trigger respiratory issues and allergic reactions (El Masri and Rakha, 2020). Furthermore, seepage can pose the risk of electrical fires and shocks in the building. Extreme seepage not only creates serious problems in loss of water, but also threatens the competency and integrity of the building. Persistent water invasion weakens the materials used in the construction of a building and leads to decreased structural integrity. This structural damage can result in costly repairs and, in severe cases, in catastrophic failures endangering lives. Studies have shown that seepage can corrode steel reinforcements, cause spalling of concrete and lead to the formation of cracks, further exacerbating the problem (Zahid et al., 2021; Zhang et al., 2023).

It is impractical to use destructive conventional methods for examining seepage-prone regions due to the large sampling area and high cost (Ramteke, 2013; Chaudhary, 2013). Al-Omosh et al. (2008) used a conventional geological survey to detect the leakage in the Bayer dam in Jordan. In another study conducted by Aufleger et al. (2007), distributed fibre optic temperature (DFOT) measurement was found suitable for detecting leakage and concrete temperatures in dams. Non-destructive testing (NDT) techniques are gaining a lot of popularity in evaluating urban infrastructures as essential tools for delivering a more comprehensive survey (Barreira and de Freitas, 2007; Martinho and Dionísio, 2014; El Masri and Rakha, 2020). Hence, geophysical investigations are necessary to delineate the potential seepage zone.

Geophysical techniques are utilized for their low cost, time efficiency and ability to detect anomalous zones precisely. In recent years, out of many NDT techniques, ground penetrating radar (GPR) has been utilized to identify defects in concrete structures of urban areas (Bellanova et al., 2020; Li et al., 2021; Yan et al., 2022). GPR is efficient in delineating water seepage by inspecting images (radiograms) of distinctions between the leaking water and the surrounding soil resulting from changes in dielectric properties (Halimshah et al., 2015; Aslam et al., 2022). GPR methods are innovative, non-invasive tools to identify seepage-prone zones accurately and efficiently, addressing critical issues and challenges emerging in urban infrastructure. The potential of GPR coupled with other techniques, like spectrometers/infrared cameras, Electrical Resistivity Tomography (ERT) and Electromagnetic Induction (EMI), have been demonstrated for several other applications around the world (Panisova et al., 2013: Bellanova et al., 2020; Hussain et al., 2020; Aslam et al., 2022; Carrive et al., 2022; Pena et al., 2023). The Self-Potential (SP) method, one of the oldest geophysical methods, is established on the existence of electrical fields naturally on the surface of the earth (Jouniaux et al., 2009). It is a passive electrical technique that involves the measurement of electrical potential by flowing water within a structure or sub-surface. In conjunction with other geophysical techniques, SP method-based surveying is effective, particularly for localizing and quantifying groundwater flows and the propagation of contaminant plumes, as well as evaluating the relevant hydraulic parameters of aquifers (Panthulu et al., 2001; Jouniaux et al., 2009). GPR, on its own, is used to study and map the voids under concrete slabs, mapping of reinforcement bars, … etc. Similarly, the SP method is also used individually to detect seepage paths. A detailed description of the combined use of GPR with other geophysical NDTs is reported by Elseicy et al. (2022) to extend its capabilities.

All the studies mentioned above exhibited the suitability of using GPR with other geophysical techniques, but no studies accounted for its use in combination with the SP method in detecting seepage-prone regions. This is the first ever reported use of an innovative combination of GPR and SP methods to detect the seepage-prone regions in the basement of a building and probable source points. In the present case, these two methods were combined to detect defects as well under concrete associated with seepage. This work will be of great significance in demonstrating the utilization of non-destructive and economical geophysical techniques for extracting information about seepage-prone zones in the basement of an urban building.

Study Site

The test site is a basement of a building in Chennai district, India (Figure 1). Structural cracking was seen at four locations within the body of the slab of the basement. Water started to pour into the basement and the elevator pits only after a year of tenancy of the building complex. The water leakage in the basement slab through cracks and expansion joints has made the parking garage less usable. The soil layers of the site are composed of medium-density to thick-silty sand in the top 5 m, with a Standard Penetration Test (SPT) 'N' range of 10 to 15. The foundation slab of reinforced concrete raft base has a thickness of 1200 mm.

Figure (1): Water leakage in the basement slab of the building

MATERIALS AND METHODS

In the present study, two types of GPR instruments (Zond 12e, proceq) were used along with an SP setup (porous pot, multimeter, copper rod, copper-sulphate solution) to acquire data. The detailed specifications of the instruments are mentioned in Table 1 and Table 2. A geological study of the area confirmed the concrete as the primary composition material of the basement. A total of 115 blocks of data have been acquired in grid format to cover the entire basement.

Table 1. Specifications of proceq sub-surface GS 8000

Proceq Sub-surface GS 8000	
Frequency Range	40 – 3440 MHz (modulated)
Acquisition Modes	Line scan, Area scan, Free path
RADAR Technology	Stepped frequency continuous-wave GPR
Maximum Depth Penetration	~ 10m
Antenna Positions	Ground coupled with dual axis floating
Wheel Encoders	2
GNSS Receiver	Available
Connectivity	Wi-Fi, Ethernet, USB-A, USB-B, USB-C

Table 2. Specifications of zond-12e advanced GPR

Zond-12e Advanced GPR	
Frequency Range	300 MHz (used here)
Number of Channels	2
Frequency of Pulse Repetition of Transmitter	82 kHz
Scan Rate	80 scans per second
Samples per Scan	128 x 16 bit
Filters	High-pass filter (used here)
Data Transmission	Wi-Fi or Ethernet to PC

GPR Surveying

For surveying, grid spacing is chosen based on the expected size of an anomaly in the case of localized targets and resolution requirements. The GPR survey was performed in 1x1 m grid mode (Figure 2). GPR transmits the electromagnetic (EM) waves into the ground and receives back the reflected signals reaching the surface and records in time: voltage signal ratio. The interaction of EM waves with any material is affected by the dielectric properties of that material. Dielectric permittivity is defined as the ratio of electric field within a material and related electric displacement. It is a diagnostic physical property for GPR, as it affects the wavelength, velocity and attenuation of propagating EM waves through a material. Relative permittivity is used to express the dielectric properties of materials relative to that of free space.

The increase in conductivity or frequency increases the attenuation, as it is the function of frequency, permittivity and conductivity. An increase in conductivity leads to deterioration in the resolution of received signals, as the GPR reflections are strongly dependent on the conductive properties of the material. Moreover, magnetic permeability describes the response of a material to the propagating GPR wave due to the action of EM fields on the spin of permanent magnetic dipole moments in the material. It impacts the reflection, refraction and velocity of radio-wave signals as they propagate through the earth. For a material to become ‘magnetic’ enough to affect the propagation and attenuation of the GPR wave, it must typically contain more than about 10%-20% by volume of magnetic minerals. Such materials are uncommon, but can be found in iron-rich sands, rusting steel-reinforced concrete, some magnetite-rich igneous rocks and concrete/building products that are made from iron smelting waste. High-quality data was recorded carefully by choosing the parameters, such as sample/scan and right frequency antenna, to retrieve optimal output as per depth of interest and required resolution at the time of GPR-data acquisition. The selection of parameters is important during GPR surveying. The understanding and choice of these parameters play a significant role in obtaining high-quality GPR data. The choice of antenna frequency is crucial, as it determines the depth of penetration and the resolution of the GPR data. Lower frequencies (e.g. from 100 MHz to 250 MHz) provide deeper penetration but lower resolution and are suitable for detecting larger objects or features deeper underground. Higher frequencies (e.g. 500 MHz to 1 GHz) offer higher resolution, but shallower penetration, ideal for detailed imaging of smaller features closer to the surface. The specific frequency should be chosen based on the depth of interest and the size of the features expected to be detected. Parameters for data processing, such as filtering and gain settings, should be carefully chosen to enhance the visibility of relevant features without introducing artefacts. Post-acquisition, the following processing steps were applied to the recorded GPR data using prism and slice software.

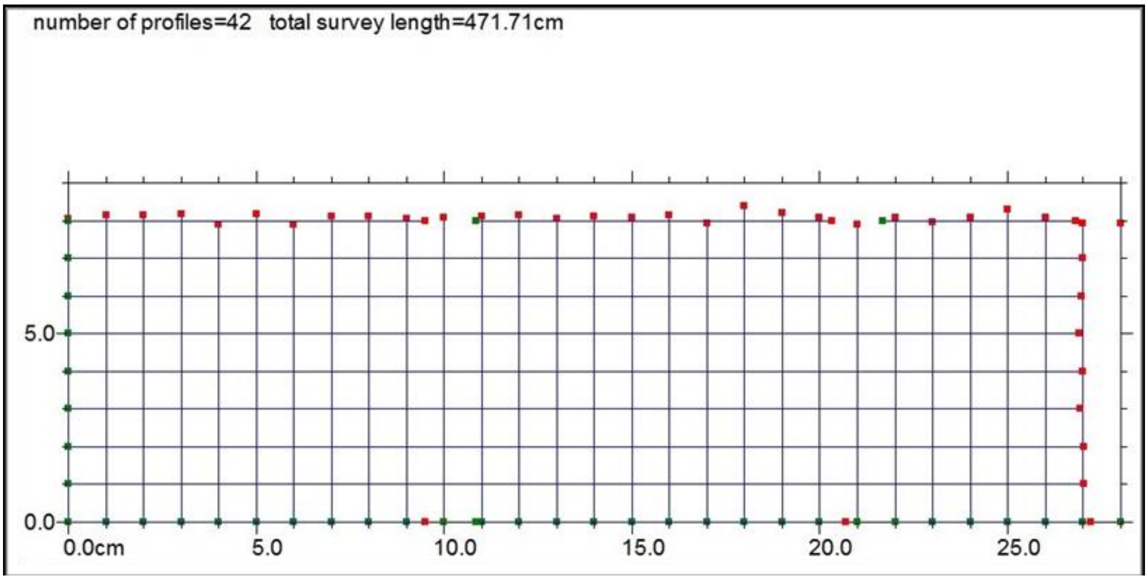

Figure (2): GPR survey with grid size of 1x1 m

1. Linear interpolation is applied to correct the changes in the speed of data acquisition, which is inevitable while working manually.
2. DC shift correction is done to remove trace samples before time-zero or first-wave arrival.
3. The accurate time of signal propagation between transmitting and receiving antennas is obtained by applying the time-zero correction method.
4. The background signals which may be seen on the profile as horizontal lines are removed to ensure efficient background suppression. The algorithm of background suppression consists of summation and normalization to calculate the averaged trace profile. It is then subtracted from every single trace of the original profile.
5. The horizontal low-pass filter is applied to suppress the fast signal variables and extract slow signal variables from layer limits. This step confirms that the averaged trace replaces the trace from the input profile in a known window which is in the middle location. Therefore, the obtained resultant trace is recorded in an appropriate position of profile. The width of the window is an input parameter for this filtering process.
6. Ormsby band-pass filter acts along a trace. It is applied for the interference of low-frequency and suppression of high-frequency components of the signal. It is applied here in three steps: (1) Transition from the time domain into the frequency domain using the direct fast Fourier transform (FFT) method; (2) Suppression of low-and high-frequency components of trace spectrum; (3) Transition from the frequency domain into the time domain using reverse FFT. The suppression/pass frequencies in the low-and high-frequency regions of

the frequency axis are used as input parameters during this process. The required frequency-response setup of a filter is achieved by moving cut-off and bandwidth frequencies on the frequency axis.

7. Migration-based signal processing filter is used firstly by fitting a hyperbola to match that observed on the raw radargrams. The hyperbola is then utilized through the radargram by adding all the waves that fall along the hyperbola and the resultant wave is located at its vertex. Kirchhoff migration was used here for processing to make variations on hyperbolic summation.
8. Hilbert transform is applied to access the slices narrower than the size of the antenna wavelet. Within the window shorter than the wavelet, the creation of time slices from the raw pulses radargram can give slices with noises. This is due to the location of a slicing window over the pulse's phase near zero. Hilbert transform of the signals of raw pulses near the 0 phase would illustrate a strong reflection close to the signal peak.

SP Method

SP is the occurrence of electrical potential naturally on the earth rising from geologic, geochemical and hydrologic interactions. However, it played a vital role in this work in identifying the seepage and moisture zones. These potentials are measured in millivolts (mV) comparative to a "survey base", wherever the potential is randomly given to be zero volts.

SP survey consists of three porous pots with copper rods in each pot and filled with copper-sulphate solution for ionic exchange between the ground and the pot. Three pots are termed as base pot, infinitive pot and roving/moving pot. The base pot and the infinitive pot remain at a constant position for the entire survey, while the roving pot is placed at every 2-m interval to calculate the potential difference (Figure 3). The usage of the infinitive pot is to measure the telluric current which alters with that of earth's magnetosphere at different parts of the day. A total of 130 SP lines have been performed to cover the entire area. Readings are recorded with the defined sign convention.

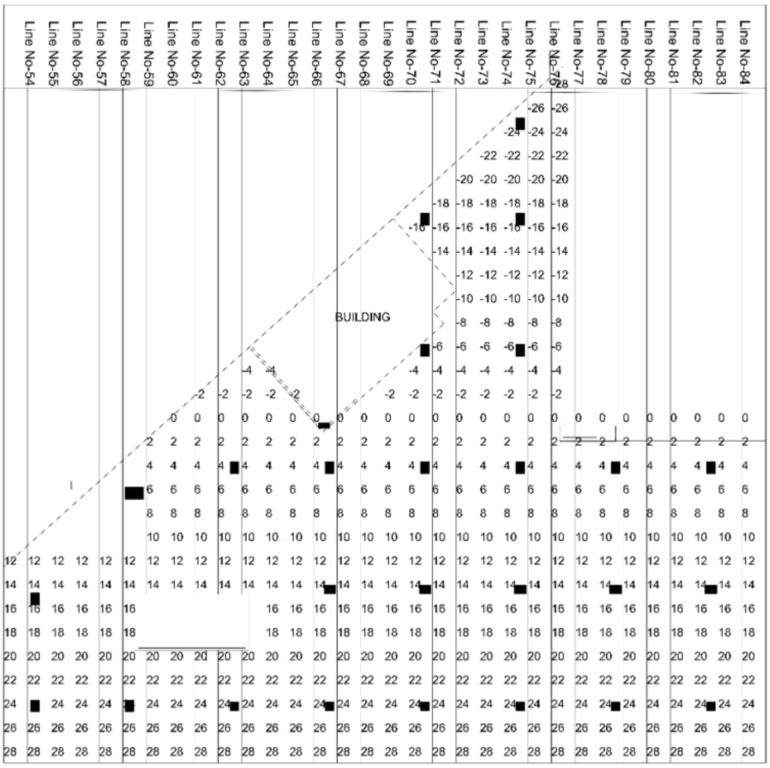

Figure (3): SP with 2-m spacing

In this survey, two values must be noted, the potential difference between base pot and infinitive pot (infinitive value) and the potential difference between base pot and roving pot (SP value). Before initiating the survey, the potential difference between base pot and roving pot is measured in a bucket filled with copper-sulphate solution and the same is repeated at the end of the survey. The difference should be subtracted from the final SP value to eliminate the pot drift. Both infinitive and SP values are noted for every 2-m interval. Post-data acquisition, the infinitive value and the pot-drift value are subtracted from the SP value to determine the final SP value of the point location. The same is being repeated for the entire survey line. The same is being repeated for all 130 lines with 2-m interval spacing. Then, the 2D section of the SP survey was created with the Surfer 13 software which produced a reliable result for correlating and interpreting GPR results. The SP values are obtained at different chainages. Factors like Telluric current, error in polarity, cultural noise because of power lines, metal pipes, drill holes, … etc. and electrode problems due to chemical differences, sunlight, temperature, pot drift or soil moisture significantly affect SP values. The methodology flow chart adopted in this study is given in Figure 4.

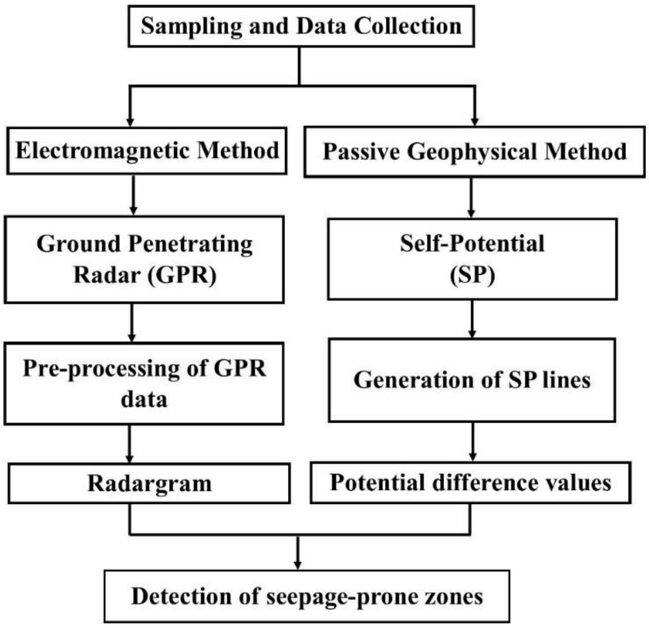

Figure (4): Methodology flowchart

RESULTS AND DISCUSSION

Since it is an integrated approach of GPR & SP to detect the seepage zones, the interpretation is performed on the correlation between both the survey results. No anomaly was marked based on the results of any one survey. For better visualization, all 2D radargrams of a block were combined to produce a 3D model using GPR Slice software to distinguish various features at different depths. EM velocity determination was carried out by fitting synthetic-hyperbola to observed-hyperbola signatures and a relative permittivity of 6 to 9 was used for time-depth conversions. The warm colors in depth slices show a high amplitude of return signal, which will happen only due to the presence of an interface across which there is a contrast in dielectric constant (relative permittivity). In GPR results, it's not always possible to determine the bottom of a feature due to the presence of ringing/echo/reverberations from the top of anomalies. It should therefore not be attempted to determine bottom of anomalies from GPR data. GPR results show the mixture of high- and low-amplitude reflections; high amplitude represents water-saturated zone, whereas low amplitude depicts the moistured zone. In highly moistured zone or in the water-seepage zone, high positive SP values are observed as the water traverses *via* pores and cracks in concrete in an upward direction towards the ground surface. The movement of water in pores indicates the exchange of ions, thereby inducing a potential which is measured using the respective apparatus. The SP value tends to remain the same regardless of the direction of the survey performed. The visualization of GPR depth slices for the sample block is shown in Figure 5. Red color shows zones with the highest amplitude and blue color shows zones with the least amplitude. The GPR grid for the sample block is represented in Figure 6. The locations of a zone of interest (ZOI) after correlating GPR and SP results for the sample block are shown in Figure 7.

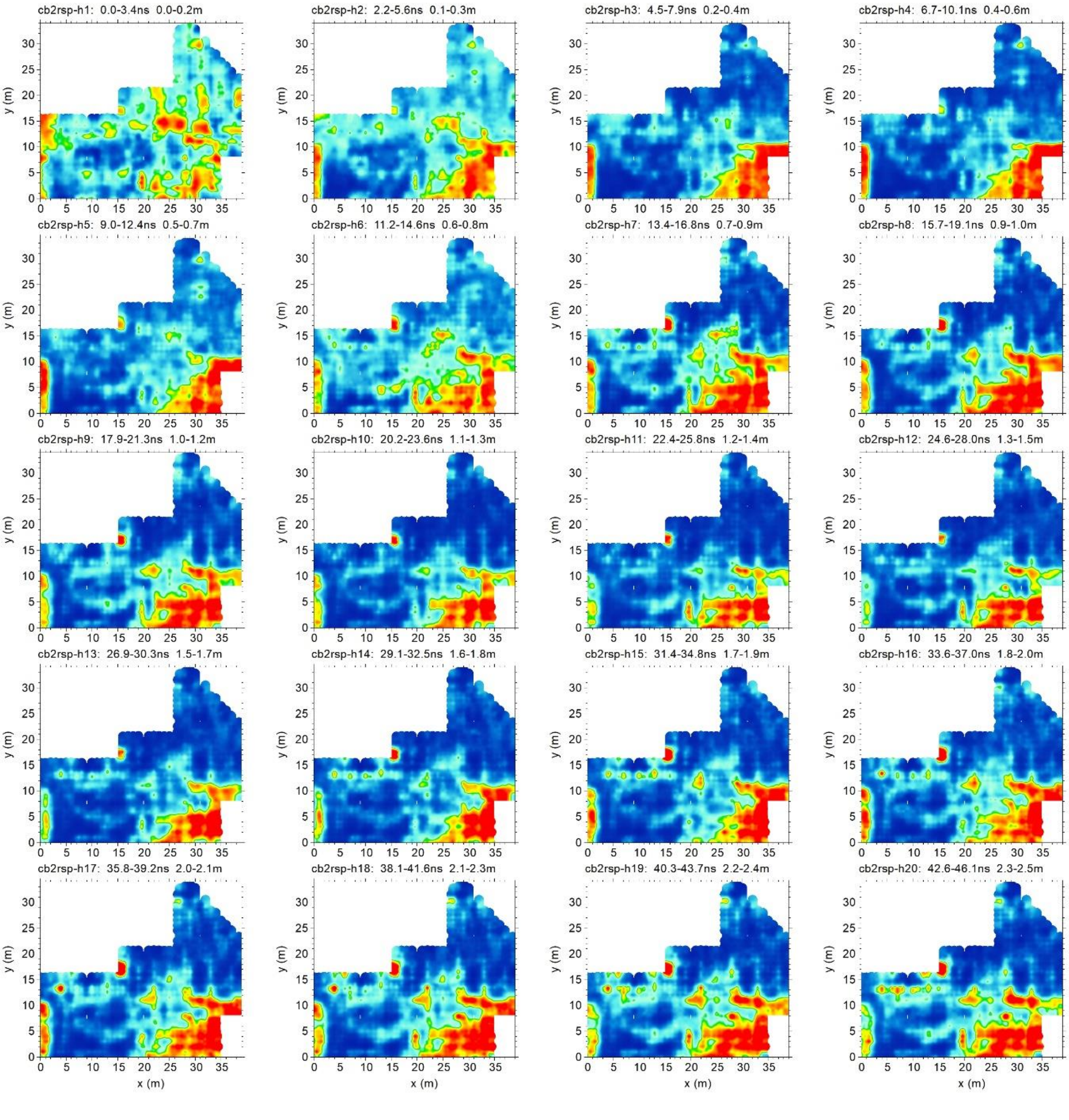

Figure (5): Visualization of GPR depth slices for the sample block

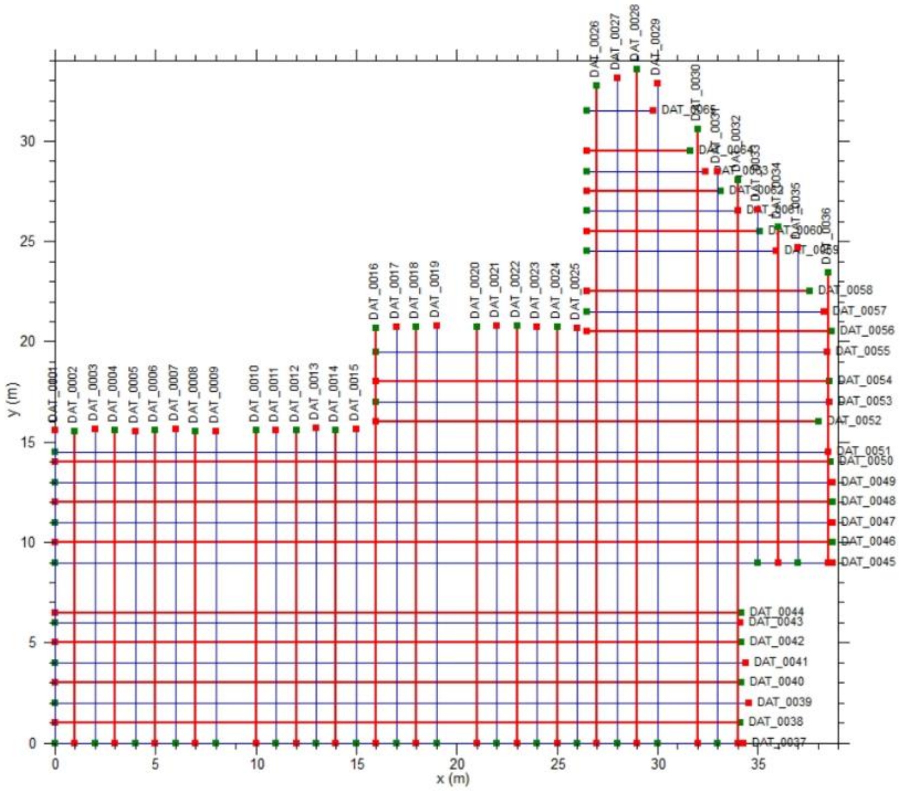

Figure (6): GPR grid for the sample block

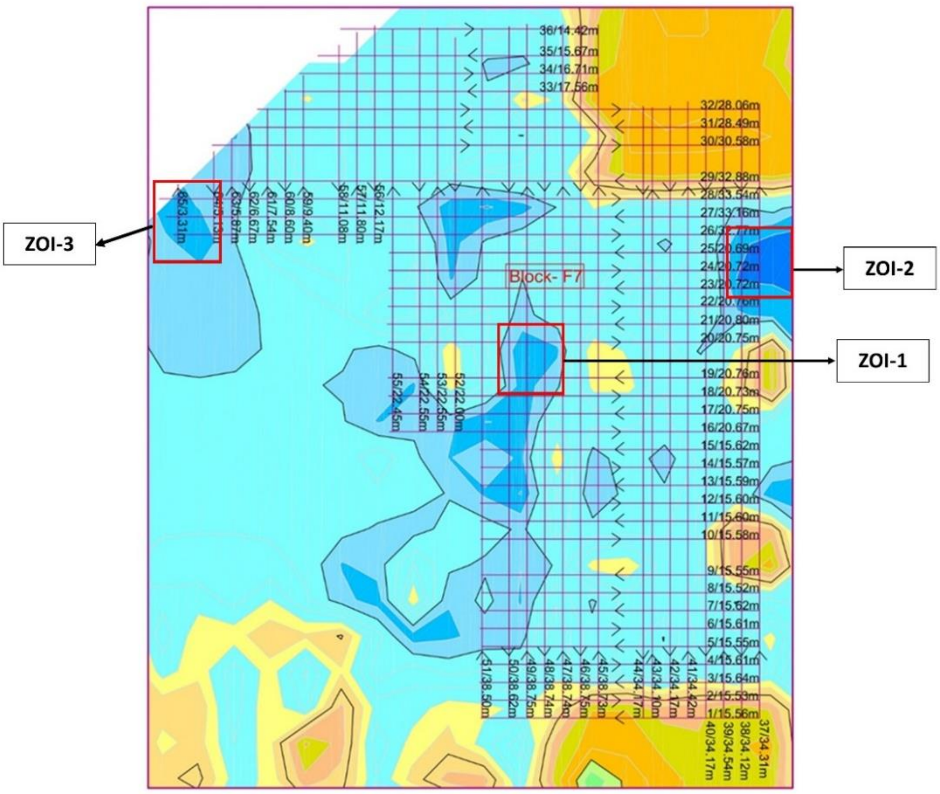

Figure (7): SP results shown over the GPR grid

In Figure 8, the images represent an extended high-amplitude zone which can be due to the high water saturation in concrete slabs extending to a depth of 1.3m below the ground. The zone is positioned 22m along the x-direction and 11m from the y-direction. This high-amplitude zone also matches with SP high-millivolt zone and hence is marked as an anomaly.

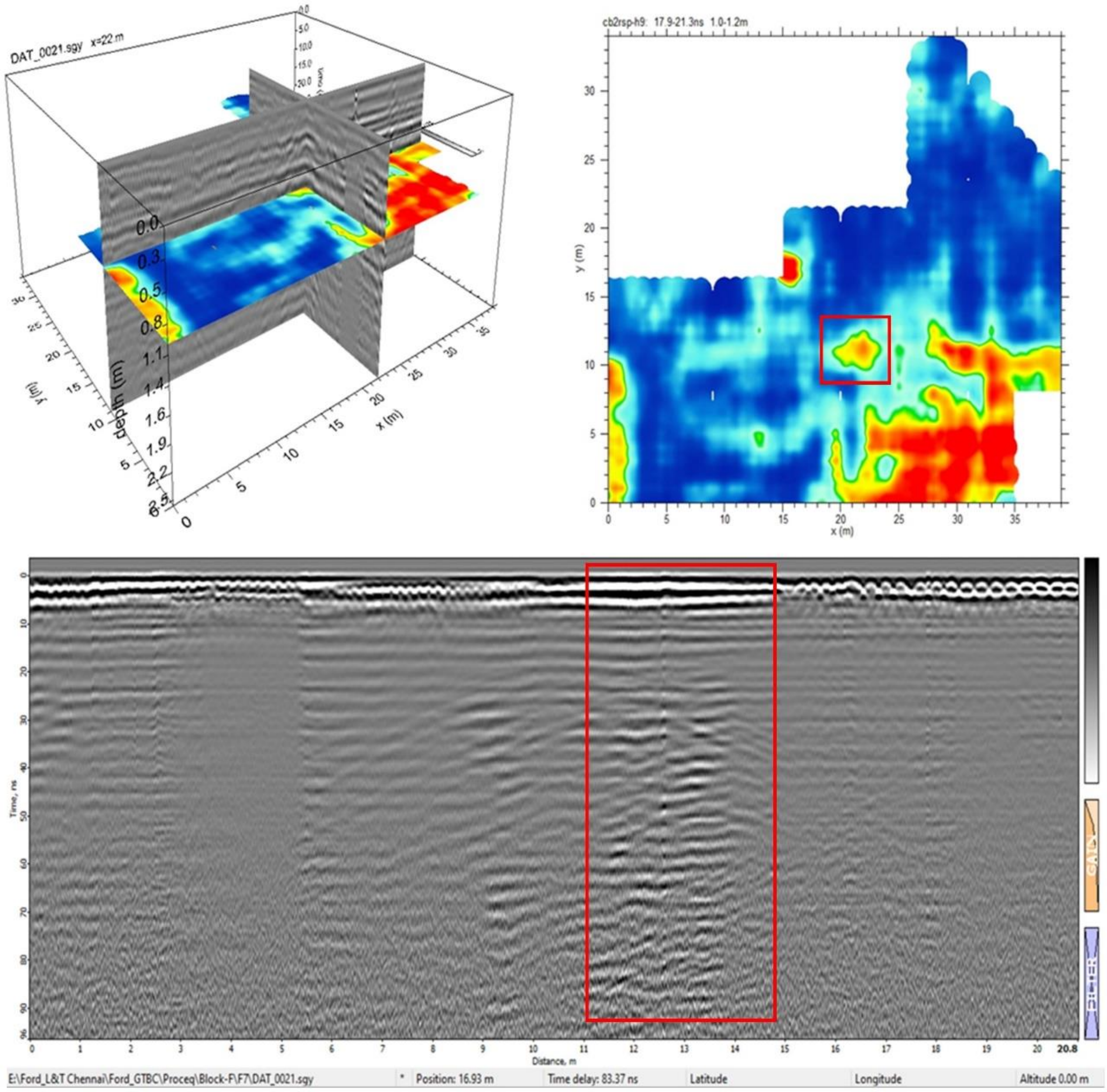

Figure (8): 3D slice highlighting ZOI-1 anomaly followed by the same anomaly in 2D radargram

As the high-saturation zone reflects most of the electromagnetic waves, it is depicted as a high-amplitude zone. The ZOI-2 is positioned at 0-5m along the y-axis and 22-28m along the x-axis. The zone marked in a red square also relates to the high-millivolt SP zone and is so marked as an anomalous portion (Figure 9). This high-saturation zone perhaps can be a source point, as a high reflection is observed.

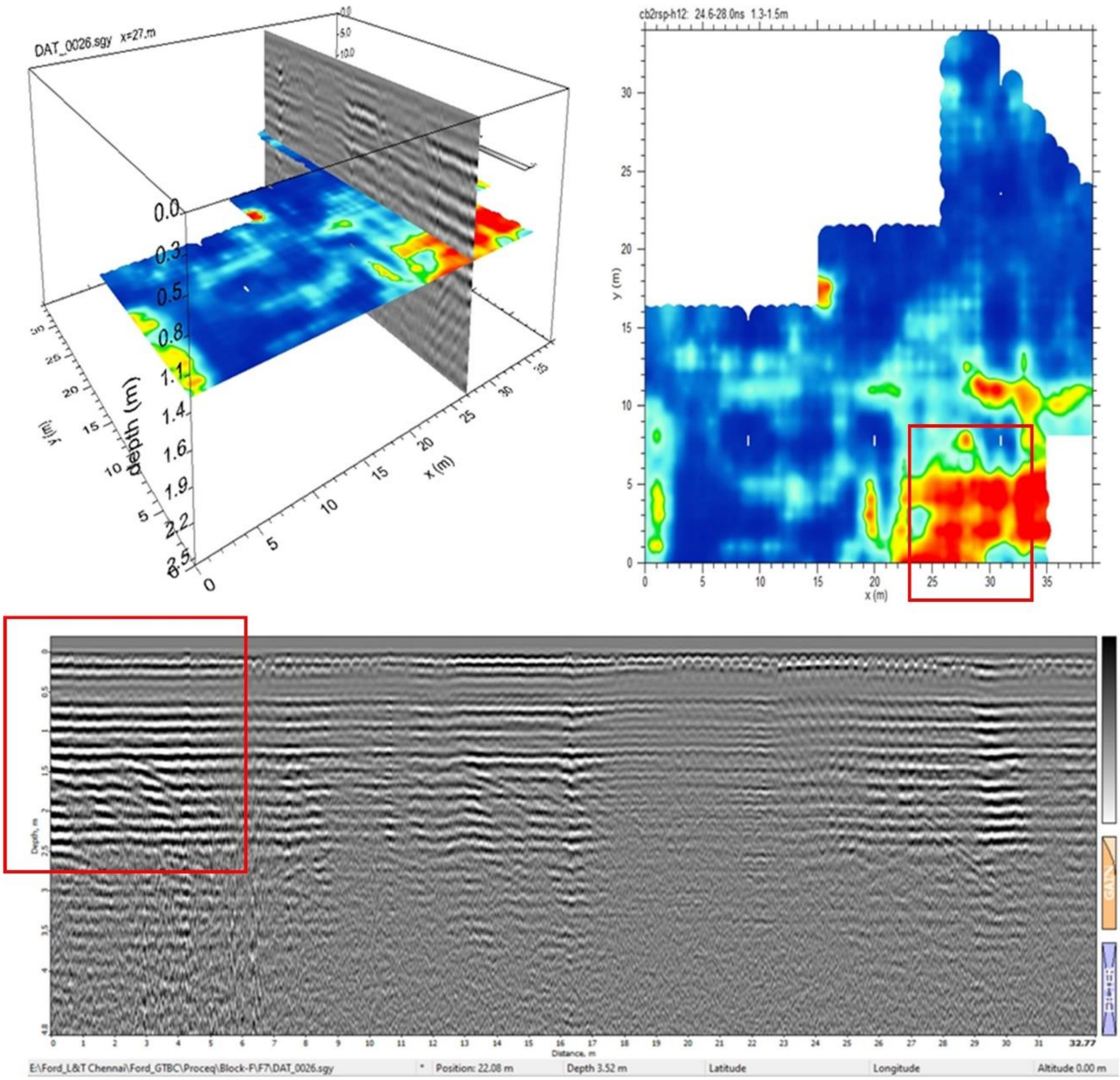

Figure (9): 3D slice highlighting ZOI-2 anomaly followed by the same anomaly in 2D radargram

The intense blue portion indicates the moisture content in the concrete slab which in turn deteriorates the EM waves, thus receiving a weak-amplitude signal. The major portion of sample block 1 is moisture which can be depicted clearly from the above image and matches with the SP results making more of a more promising interpretation. The zone marked in red square shows the change in intensity with the surrounding zones and matches with the high-millivolt SP zone, thus marked as an anomaly. The zone is positioned 30-34 m along the y-direction and 26-28 m along the x-direction. The 2D radargram of the ZOI-3 anomaly is shown in Figure 10.

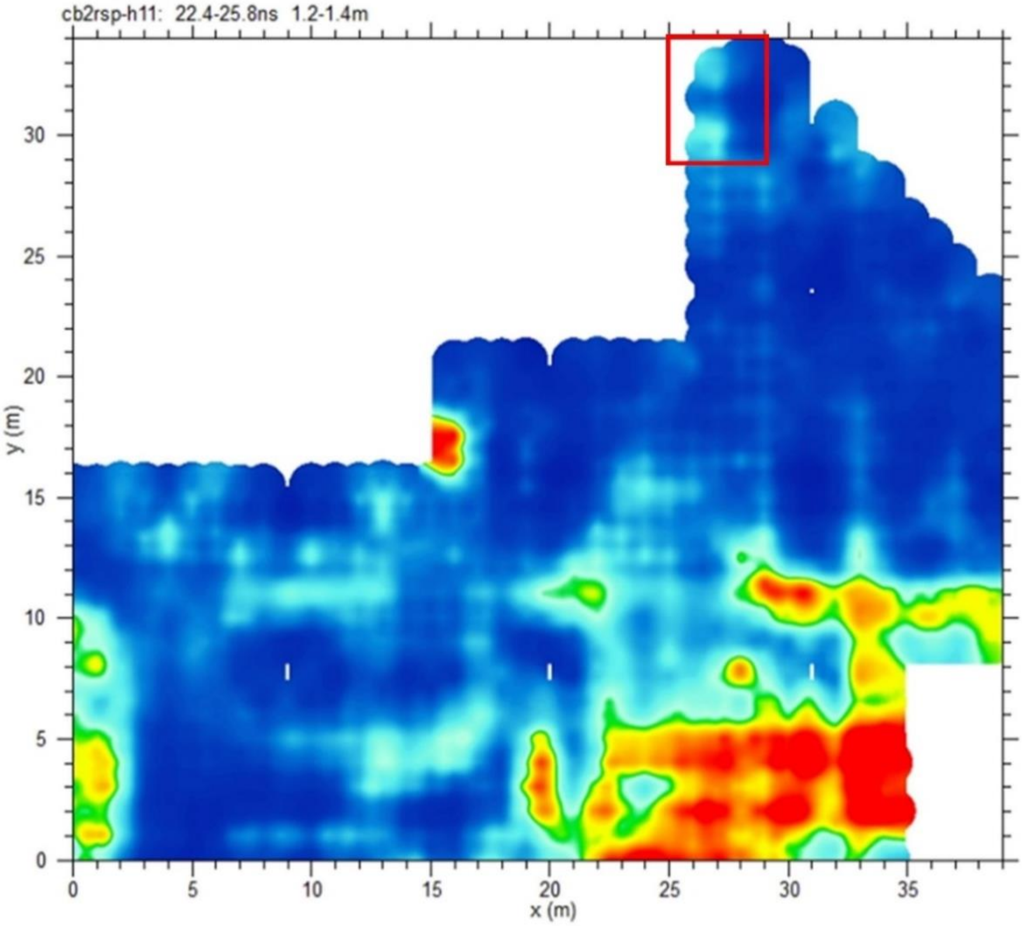

Figure (10): ZOI-3 anomaly in 2D radargram

Although the results of this study exhibited high effectiveness of the combined method of GPR and SP for conducting a rapid inspection of seepage-prone regions and possible source points in a building, the potential limitations of the study are as follows:

1. **External factors:** The study might not account for all potential external factors that could influence seepage, such as recent weather conditions, nearby construction or underground infrastructure.
2. **Temporal factors:** The study's findings are based on data collected at a specific time. Seepage patterns and intensities can change over time and the study might not capture these dynamics.
3. **Depth of investigation**: The depth to which GPR and SP methods can effectively detect anomalies may be limited, potentially missing deeper seepage sources.
4. **Technology constraints:** The study is constrained by the current state of technology in GPR and SP methods, which may evolve and provide more accurate data in the future.
5. **Complexity of seepage phenomena:** Seepage is a complex phenomenon influenced by various factors (e.g. soil composition, water-table level, structural integrity). The study may not fully account for this complexity.

CONCLUSIONS

An integrated geophysical investigation was carried out using GPR and SP surveys at proposed locations for successfully determining the seepage zones. The integration of these geophysical techniques is used to carry out investigations at the study site, where non-destructive techniques cannot be performed. The conclusions based on the current-study findings are as follows:

(1) In highly moistured and water-saturated zones, the high positive SP values have been generated and for GPR low-amplitude and high amplitude are

produced respectively based on the water quantity that the location holds.

(2) Anomaly is finalized only after observing both SP and GPR results, thus ensuring the reliability of the interpretation. Anomalies of GPR have been both high-amplitude and low-amplitude zones, as the completely water-saturated concrete blocks reflect the EM waves due to high contrast in their dielectrics, thus depicting a high-amplitude zone and the zone which is partially moistured allowing the waves to pass by, but the attenuation of waves is high, which portrays as low-amplitude zones.

(3) In SP, when the water moves through the pores and cracks the concrete block towards the surface, it has a positive SP value and *vice versa*. The investigation clearly brings out the location of seepage/moistured points, with an excellent correlation between the GPR and SP surveys conducted.

Moreover, using state-of-the-art geophysical techniques to detect seepage-prone regions has significant practical and economic benefits for detailed investigations of a building followed by reduction in the maintenance expenditure.

REFERENCES

Al-Omosh, H., Al-Farajat, M., and Franz Zunic, F. (2008). “Leakage in bayer dam in Jordan: Its causes and consequences”. Jordan J. Civ. Eng., 2 (4), 363-376.

Aslam, H., Mortula, M.M., Yehia, S., Ali, T., and Kaur, M. (2022). “Evaluation of the factors impacting the water-pipe leak-detection ability of GPR, infrared cameras and spectrometers under controlled conditions”. Appl. Sci., 12, 1683.

Aufleger, M., Conrad, M., Goltz, M., Perzlmaier, S., and Porras, P. (2007). “Innovative dam-monitoring tools based on distributed temperature measurement”. Jordan J. Civ. Eng., 1 (1), 29-37.

Barreira, E., and de Freitas, V.P. (2007). “Evaluation of building materials using infrared thermography”. Constr. Build. Mater., 21, 218-224.

Bellanova, J., Calamita, G., Catapano, I., Ciucci, A. et al. (2020). “GPR and ERT investigations in urban areas: Case study of Matera (southern Italy), Remote Sens., 12, 1879.

Carrive, P., Saintenoy, A., Léger, E., Arcone, S.A., and Sailhac, P. (2022). “Exploiting ground-penetrating radar signal enhancement by water-saturated bulb surrounding defective water pipes for leak detection”. Geosciences, 12, 368.

Chaudhary, M.T.A. (2013). “Structural condition assessment and functional appraisal of a large basement affected by groundwater leakage”. Eng. Struct., 52, 384-393.

El Masri Y., and Rakha, T. (2020). “A scoping review of non-destructive testing (NDT) techniques in building performance diagnostic inspections”. Constr. Build. Mater., 265, 120542.

Elseicy, A., Alonso-Díaz, A., Solla, M., Rasol, M., and Santos-Assunçao, S. (2022). “Combined use of GPR and other NDTs for road-pavement assessment: An overview”. Remote Sens., 14, 4336.

Halimshah, N.N., Yusup, A., Amin, Z.M., and Ghazalli, M.D. (2015). “Visual inspection of water leakage from ground-penetrating radar radargram: ISPRS ann”. Photogramm. Remote Sens. Spat. Inf. Sci., II (w2), 191-198.

Hussain, Y., Uagoda, R., Borges, W., Nunes, J., Hamza, O. et al. (2020). “The potential use of geophysical methods to identify cavities, sinkholes and pathways for water infiltration”. Water, 12, 2289.

Jouniaux, L., Maineult, A., Naudet, V., Pessel, M., and Sailhac, P. (2009). “Review of self-potential methods in hydrogeophysics”. C.R. Geoscience, 341, 928-936.

Li, S., Gu, X., Xu, X., Xu, D., Zhang, T., Liu, Z., and Dong, Q., (2021). “Detection of concealed cracks from ground-penetrating radar images based on deep-learning algorithm”. Constr. Build. Mater., 273, 121949.

Martinho, E., and Dionísio, A. (2014). “Main geophysical techniques used for non-destructive evaluation in cultural built heritage: A review”. J. Geophys. Eng., 11, 053001.

Panisova, J., Frastia, M., Wunderlich, T., Pasteka, R., and Kusnirák, D. (2013). "Microgravity and ground-penetrating radar investigations of sub-surface features at the St Catherine's Monastery, Slovakiaa". Archaeol. Prospect., 20, 163-174.

Pena, R.W.T., Oliva, P.A.C., and Abrunhosa, F.A. (2023). "Application of the ground-penetrating radar (GPR) and electromagnetic (EM34-3) geophysical tools and sedimentology for the evaluation of the sub-surface of sites earmarked for aquaculture ponds in the Amazon region of northern Brazil., Appl. Sci., 13, 11107.

Ramteke, R.S. (2013). "Geophysical investigations for solving seepage problems". J. Indian Geophy. Union, 17 (2), 187-194.

Yan, Y., Yan, Y., Zhao, G., Zhou, Y., and Wang, Z. (2022). "Combined ERT and GPR data for sub-surface characterization of weathered hilly slope: A case study in Zhejiang province, southeast China". Sustainability, 14, 7616.

Zahid, H.F., Jiradilok, P., Kuntal, V.S., and Nagai, K., (2021). "Investigation of the effects of multiple and multi-directional reinforcement on corrosion-induced concrete cracking pattern". Constr. Build. Mater., 283, 122594.

Zhang, J., Li, J., Zhao, Y., Wang, S., and Guan, Z. (2023). "Concrete-cover cracking and reinforcement corrosion behavior in concrete with new-to-old concrete interfaces". Materials, 16, 5969.